Available online at www.sciencedirect.com
ScienceDirect
Solar Energy 84 (2010) 792–800
SOLAR ENERGY
www.elsevier.com/locate/solener

Optical design of a high radiative flux solar furnace for Mexico

D. Riveros-Rosas [a], J. Herrera-Vázquez [b], C.A. Pérez-Rábago [a], C.A. Arancibia-Bulnes [a,*], S. Vázquez-Montiel [b], M. Sánchez-González [c], F. Granados-Agustín [b], O.A. Jaramillo [a], C.A. Estrada [a]

[a] Centro de Investigación en Energía, Universidad Nacional Autónoma de México, Av. Xochicalco s/n, A.P. 34, Temixco, 62580 Morelos, Mexico
[b] Instituto Nacional de Astrofisica, Óptica y Electrónica, Luis Enrique Erro 1, Tonantzintla, A.P. 216, 72000 Puebla, Mexico
[c] Centro Nacional de Energías Renovables, Calle Somera 7-9, 28026 Madrid, Spain

Received 23 August 2009; received in revised form 2 February 2010; accepted 9 February 2010
Available online 19 March 2010

Communicated by: Associate Editor L. Vant-Hull

Abstract

In the present work, the optical design of a new high radiative flux solar furnace is described. Several optical configurations for the concentrator of the system have been considered. Ray tracing simulations were carried out in order to determine the concentrated radiative flux distributions in the focal zone of the system, for comparing the different proposals. The best configuration was chosen in terms of maximum peak concentration, but also in terms of economical and other practical considerations. It consists of an arrangement of 409 first surface spherical facets with hexagonal shape, mounted on a spherical frame. The individual orientation of the facets is corrected in order to compensate for aberrations. The design considers an intercepted power of 30 kW and a target peak concentration above 10,000 suns. The effect of optical errors was also considered in the simulations.

Keywords: Solar concentration; Segmented concentrator; Radiative flux; Solar furnace; Solar chemistry

1. Introduction

Modern solar furnace technology starts in the 1950s decade. The first research in these devices was directed towards studying the effects of high temperatures (around 3500 °C) on the properties of different materials exposed to highly concentrate solar fluxes (Glaser, 1958). Among their applications is the study of properties like thermal conductivity, expansion coefficients, emissivity, melting points (Hisada et al., 1957), and also the study of ultra refractory materials, determination of phase diagrams, crystal growth, and purification of materials. At the same time, methods for the measurement of high temperatures in receivers (Brenden et al., 1958), and the flux density of concentrated radiation (Loh et al., 1957) have been developed. The later have evolved and image digitalization techniques are used (Jonhnston, 1995), together with calorimetric techniques (Pérez-Rábago et al., 2006; Estrada et al., 2007).

Among the first furnaces built, were the furnace of Arizona State College in the USA, in 1956 (Kevane, 1957), and the furnace of the Government Institute for Industrial Research, in Japan (Hisada et al., 1957). Solar furnace technology has evolved, and larger furnaces have been built, like the one of the CNRS in Odeillo, France, with 1000 kW (Trombe and Le Phat Vinh, 1973); the furnace of the Academy of Sciences of Usbekistan, with 1000 kW (Abdurakhamanov et al., 1998); the furnace of Paul Scherrer Institute (PSI), of 25–40 kW (Schubnell et al., 1991); the furnace of CIEMAT, in Plataforma Solar de Almería, Spain, with 45 kW; and the furnace of DLR, in Cologne, Germany, of 20 kW (Neumann and Groer, 1996). More

* Corresponding author. Tel.: +52 (55) 56229831; fax: +52 (55) 56229791.
E-mail address: caab@cie.unam.mx (C.A. Arancibia-Bulnes).

0038-092X/$ - see front matter © 2010 Elsevier Ltd. All rights reserved.
doi:10.1016/j.solener.2010.02.002

recently, a designs based on nonimaging optics has been developed (Chen et al., 2002; Lim and Li, 2009)

Mexico has an ideal position for the implementation of solar technologies, due to its favorable geographical location in the sunbelt of the planet. The estimated yearly average insolation is higher than 5.5 kW h/m^2 per day over the country. In particular, in the northwestern states this insolation can reach nearly 6 kW h/m^2 and has a very important component of beam solar radiation. This high quality solar resource makes that area ideal for the implementation of concentrating solar technologies (CST), either for electrical power generation or for the production of solar fuels as Hydrogen. With the aim of promoting the development of CST in México, the construction of a high radiative flux solar furnace (HRFSF) was proposed, as a tool for research and development in the field. This development is part of a larger project known as "National Laboratory for Solar Concentration Systems and Solar Chemistry", which involves also the development of a Heliostat Test Field and a Solar Photocatalytic Water Treatment Plant. Federal funding for the development of this infrastructure was approved by Consejo Nacional de Ciencia y Tecnología (CONACYT), and the project is now in progress, with additional funding from Universidad Nacional Autónoma de México (UNAM) and Universidad de Sonora (UNISON). The HRFSF is being developed in a 3 year period, starting from September 2007, by UNAM, in collaboration with Instituto Nacional de Astrofísica, Óptica y Electrónica (INAOE), and other institutions. The main applications of this infrastructure are expected to be in the areas of solar chemistry and solar materials processing (Fletcher, 2001).

Based on the information available in the literature and with the aim of building a highly concentrating system, the design targets for the HRFSF were set as follows: thermal power of 30 kW and peak concentration above 10,000 suns, producing a solar image of 10 cm diameter or smaller. In order to achieve the above targets, several possible configurations were analyzed and the optical characteristics of the system were optimized by means of ray tracing simulations.

There is little information in the literature regarding the detailed optical analysis of the existing furnaces and discussing the considerations and methods that led to their final optical design. In order to contribute to the understanding of the effect of different parameters and their interaction on the performance of high concentration solar devices, the procedures followed in the design of the HRFSF are discussed here. In the following, the results obtained for the different studied optical configurations are presented, and the effect of the different parameters is discussed.

2. Preliminary design

The project started with an initial proposal of a furnace with around 30 kW power. The sizes of the main components were determined from this restriction, resulting in a 36 m^2 concentrator and a 81 m^2, flat heliostat, located at 14 m distance from the vertex of the concentrator. Note that, because of the low latitude of the site chosen for the furnace (the city of Temixco, in the Morelos state; at 18° 50′ 20.81″ North), as compared with other existing facilities, a large heliostat is required to fully illuminate the concentrator during a sufficient number of hours: 3 h at least in the summer solstice, and 8 h in the winter solstice. Actually, winter is the best season for experimenting with highly concentrated radiation at the site.

Some solar furnaces like those at DLR or NREL have an off-axis configuration. In the present case it was decided to use a horizontal on axis configuration instead; i.e., one with the focus in the same axis joining the center of the concentrator and the vertex of the heliostat. This kind of configuration suffers from shadowing by all the structures located in the focal region, including the positioning table, but on the other hand, reduces off axis aberration effects. The effective focal distance of the concentrator was set to 3.68 m, in order to attain a near optimal numerical aperture for the system. In general, for a faceted concentrator this optimal value differs from that for an equivalent ideal paraboloid, as has been pointed out elsewhere (Riveros-Rosas et al., 2008, submitted for publication). Actually, it has been found the optimal numerical aperture depends strongly on both the size of the facets and their optical error.

It was decided that the concentrator would be fabricated as a faceted mirror, formed by polished, first surface, glass mirrors. This kind of mirrors was chosen because they easily provide the high optical quality required for the furnace and, at the same time, they can be manufactured with very good specifications in México. Because of fabrication cost considerations, spherical curvature is chosen for the mirrors. This implies that facets are not segments of a single larger parabola, but small independent mirrors instead. The shape of the facets was chosen to be hexagonal, because this geometry fills quite well the concentrator area, still being relatively easy to polish. From the point of view of filling the space, square facets would be an interesting option also, but they are much more difficult to polish adequately.

From the results reported by Riveros-Rosas et al. (2008, submitted for publication) about the influence of the number of facets in the concentration factor, it was sought that the concentrator had the largest practical number of facets. Therefore the size of the facets was chosen to be 40 cm apothem, on the basis of local fabrication capabilities and mounting considerations.

3. Methodology

With all the above conditions established, there are still several parameters which can be optimized for the system: the spatial distribution of the facets (geometry of the sup-

porting frame), their individual inclination, and focal distances.

Regarding the first of these parameters, the geometry of the supporting structure, three different geometries were explored: flat, parabolic, and spherical. Take into account, that depending on the geometry of the mounting frame, the shape of the mirrors may be altered. For instance, in Fig. 1 it is shown how the shape of each mirror must be changed such that the hexagonal facets completely fill the surface for the spherical frame. This was done without altering the vertical dimensions of the mirrors, changing only the horizontal dimensions in order to fit the mirrors into the array. The difference with respect to regular hexagons is actually small, but it must be taken into account in the fabrication of the facets.

The other two parameters, i.e., mirror inclination and focal distances must be investigated independently for each of the three considered geometries of the mounting structure.

In the present optical system the spherical aberration of the facets is important. Due to this aberration and, to a smaller degree, to comma and astigmatism, the focal region is increased in size. Facets that are on the most external parts of the concentrator are the largest contributors to these aberrations, because radiation coming from the heliostat impinges on them at larger angles. Aberrations cannot be corrected with additional optical surfaces in a system like this. A lot of improvement can be achieved, however, by reorienting the facets to different inclinations.

In the case of the parabolic frame, the best solution is when all facets are oriented tangent to the frame; however, the spherical and flat frames require reorienting the facets. In these cases, the angle for each facet is chosen such that a light ray reflected on the center of the facet is directed towards the focal point of the system, as illustrated in Fig. 2b. This way, even though the facets are mounted on a spherical or flat frame, they are not tangent to the surface of the frame.

The third parameter to investigate is focal distance. Using different focal lengths for the facets also helps to compensate for aberrations. For this purpose, in principle, each facet should have its own focal distance. In the present case, the criterion applied was to set the focal length of each facet equal to its actual distance to the focus of the system.

One problem with the above is that fabricating many facets with different focal distances is more expensive and lengthy than making all of them equal. For that reason, the sensitivity of the design to variations in focal distance was investigated. This was done for a parabolic frame: first the reference focal length of each facet was determined with the above criterion. Then a ray tracing simulation was run for a configuration considering all those different distances. After this, the focal distances were varied: all of them reduced or increased by the same constant magnitude, from -15 to 15 cm, in 1 cm steps, and simulations were run for each configuration.

With the above procedure, it was found that focal lengths can be changed from their reference values by an amount of ± 12.5 cm (i.e., by an amount around 3.5% of the global focal length of the system) without reducing the peak irradiance by more than 3%. This indicated the feasibility of grouping facets into sets of fixed focal length. To define such groups, the following procedure was proposed: the difference between the longest and the shortest of the reference focal lengths was divided into 10 cm intervals. All the facets with focal distances falling within each interval were defined as a group. Then, the focal length

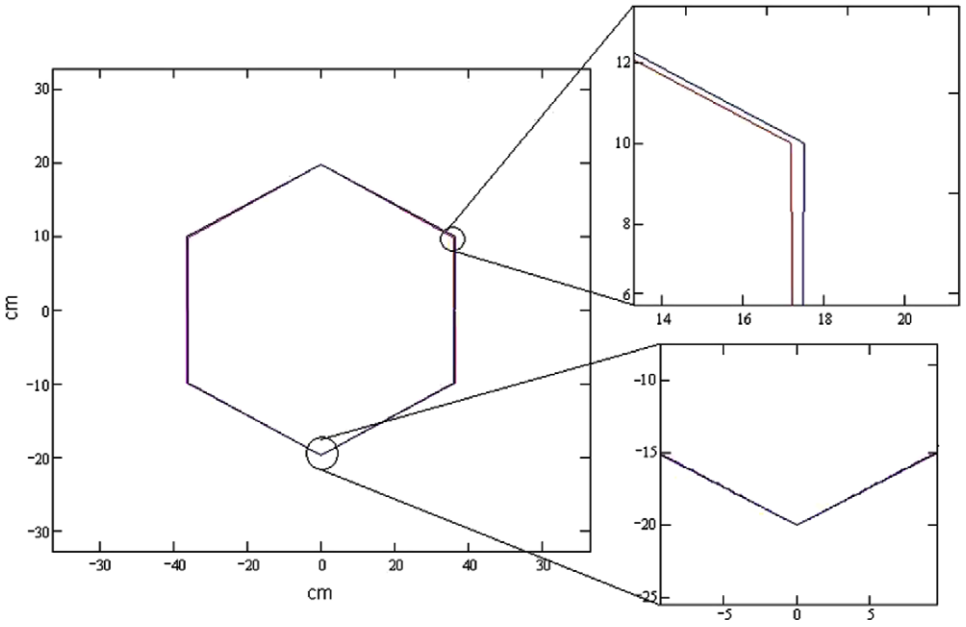

Fig. 1. Difference between the largest and the smallest hexagonal mirrors for the spherical frame.

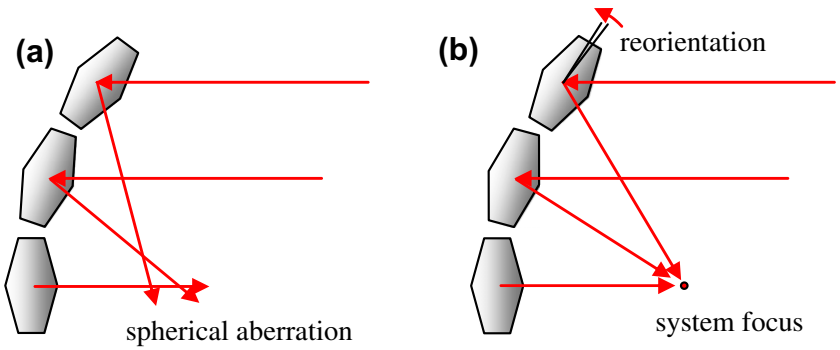

Fig. 2. Correction of spherical aberration (a) by reorientation of facets (b).

of each group was taken as the average of all the reference focal distances of the corresponding facets.

With the above procedure, the task of fabricating facets with nearly 100 different focal distances could be simplified to only around five different distances. Similar results were also obtained for the flat and spherical frames.

Based on the above arguments, the following configurations were chosen for detailed comparison, which is discussed in detail in the next section:

- P: Continuous paraboloidal mirror of square shape spanning the whole 36 m^2, as an ideal reference case.
- P1: Paraboloidal frame with tangent facets. All facets with different focal distance (reference focal lengths).
- P2: Paraboloidal frame with tangent facets. Facets in five different groups of equal focal distance.
- E1: Spherical frame with tilted facets. All facets with different focal distance.
- E2: Spherical frame with tilted facets. Facets in five different groups of equal focal distance.
- E3: Spherical frame with tilted facets. All facets with the same focal distance.
- F1: Flat frame with tilted facets. All facets with different focal distance.
- F2: Flat frame with tilted facets. Facets in five different groups of equal focal distance.
- F3: Flat frame with tilted facets. All facets with the same focal distance.

In configurations E2, P2, and F2 only five different focal distances are used, on the assumption that a good optical performance can be achieved in this way, as discussed above.

Simulations were carried out for the different configurations seeking to maximize the peak of concentration, i.e., the peak of the radiative flux distribution in the focal plane of the system. These simulations were done with a ray tracing program based on the convolution technique (Rabl and Bendt, 1982) (also known as effective source or degraded sun technique). In this technique the number of rays to be traced is very much reduced with respect to a straightforward ray tracing. This is done by performing the mathematical 2D convolution of the incident solar angular distribution (sun shape) with the global angular error distribution of the optical system. It is assumed that the optical error distribution is a normal distribution, and the measure of the global optical error is the standard deviation of this distribution. The convolution is solved numerically in order to obtain the so-called degraded sun distribution. This distribution is used as an effective solar cone in the ray tracing, accounting both for the size of the solar cone and the angular distribution of reflection errors. Finally, instead of tracing cones of radiation from the sun to the target, only the central ray of each cone is traced and the effective sunshape is projected onto the focal plane, centered on the ray impact point, in order to calculate the final irradiance distribution.

In fact, each simulation run was carried out with two ray trace codes of different nature, the first one, described in the preceding paragraph and called Tonalli (Riveros-Rosas et al., 2008, submitted for publication), is a code based on the convolution method (Biggs and Vittitoe, 1979). The second is commercial optical design software, called Zemax. It was necessary to complement this latter software with a routine in C language to calculate the irradiance distribution on the receiver.

At a first stage, optical errors were not accounted for in the simulations. Thus, the results of simulations for the different configurations investigated were compared in ideal conditions of reflectivity and specularity. From this procedure, on the basis of maximizing peak concentration, a configuration was chosen for further investigation. With this selected design, a second simulation step was carried out, by considering different values of the global optical error, in order to determine the influence of this parameter.

The global optical error takes into account all possible errors appearing in the system that affect the direction of the reflected rays: mechanical fabrication errors, facet alignment errors, heliostat tracking errors, errors in facet curvature, and intrinsic errors due to the roughness of the reflecting surface. The standard deviations of the statistical distributions for all those possible errors add in quadrature to give the global error (standard deviation of the global error function; Rabl and Bendt, 1982). The simulations allowed determining the maximum tolerable value of the global error to attain the design targets stated in the previ-

ous section. We assume, as is customary, that the error distribution corresponds to a Gaussian distribution. The global standard deviation of the optical error is varied from 2 up to 5 mrad. The sun's model was a standard solar radiation cone (Rabl and Bendt, 1982), as for instance in the CIRCE2 ray trace code (Romero, 1984). This sun shape model corresponds to an average of observations carried out with the Lawrence Berkeley Laboratories circumsolar telescope at 11 sites throughout the United States (see for instance, Buie et al., 2003).

4. Results and discussion

The main results of the simulations are presented in Table 1 and Figs. 3–7.

The highest peak concentration occurs, as expected, for the control case of a continuous paraboloid (P). An important trend to note is that using a single focal distance for all the facets gives always much worse results than using several different distances; i.e., the E3, and F3 configurations are the worst of all. However, it is also notorious that, for all different frame geometries, using just five different focal distances gives results nearly as good as using a different focal distance for each facet. This confirms the possibility of obtaining satisfactory results with a small number of different focal distances, which is cheaper to fabricate. Five or six focal distances turned out to be a good number in preliminary analyses, which is confirmed by the present results.

Another result to note is that the four configurations E1, E2, P1, and P2, are very similar to each other; there is practically no difference in peak concentration between the paraboloidal and spherical frames, either when all facets have different focal distances (E1 and P1), or when they are grouped in five sets (E2 and P2; note that the lines for these two cases are practically indistinguishable from each other in Fig. 6). Also, the cases F1 and F2 are very similar to each other. They have smaller spot radius than E1, E2, P1, and P2. However, the irradiance peak is smaller for these flat frames, as can be seen in Fig. 6.

It may seem paradoxical that the flat frame produces slightly smaller spot radius than the spherical and parabolic frames, and at the same time has lower peak concentration. However, this results means just that the flux distribution produced by the flat frame is flatter than the others, resembling more closely the sunshape, but with smaller peak irradiance. The differences come probably from the fact that in the flat configuration the facets are on the average much farther apart from the focus than in the spherical or parabolic ones. This results in longer prop-

Table 1
Results of the simulations for the analyzed configurations.

Config.	Peak flux (kW/m^2)	Spot radius (cm) 90% power	Spot radius (cm) 95% power
P	36,942	1.97	2.20
P1	34,560	2.61	3.11
P2	34,425	2.65	3.12
E1	34,548	2.63	3.14
E2	34,419	2.65	3.17
E3	29,903	2.90	3.59
F1	32,515	2.48	2.82
F2	32,316	2.52	2.89
F3	23,804	3.20	3.76

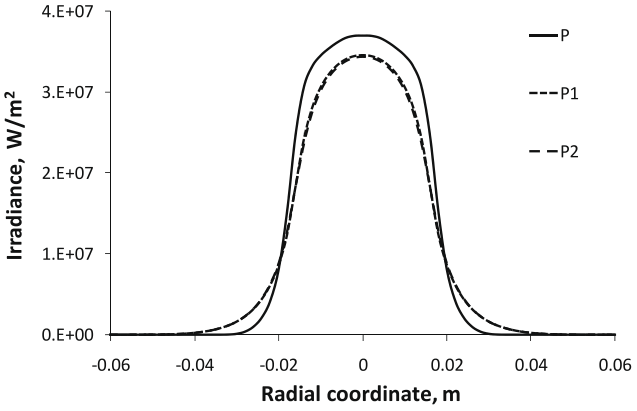

Fig. 3. Irradiance distributions in the focal plane for parabolic frame configurations, as compared to a continuous paraboloid.

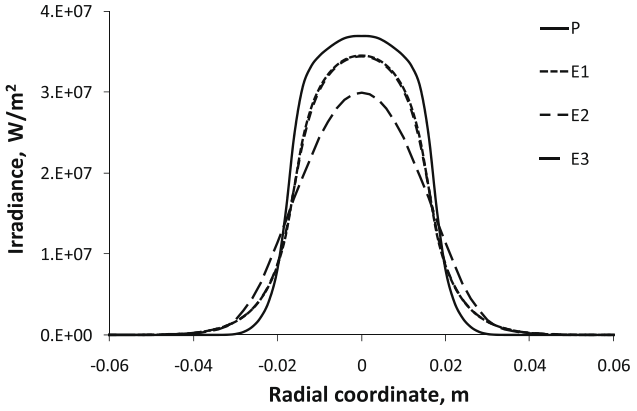

Fig. 4. Irradiance distribution in the focal plane for spherical frame configurations, as compared to a continuous paraboloid.

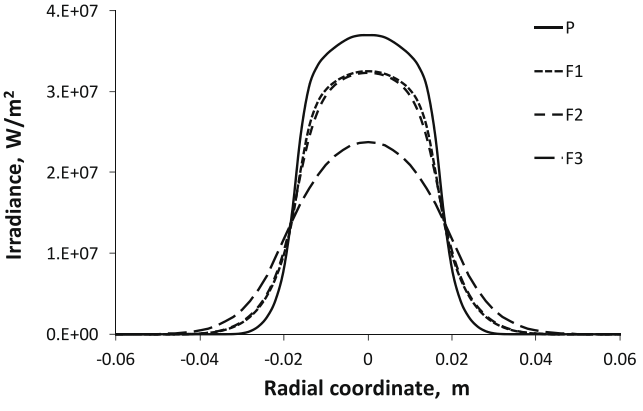

Fig. 5. Irradiance distribution in the focal plane for flat frame configurations, as compared to a continuous paraboloid.

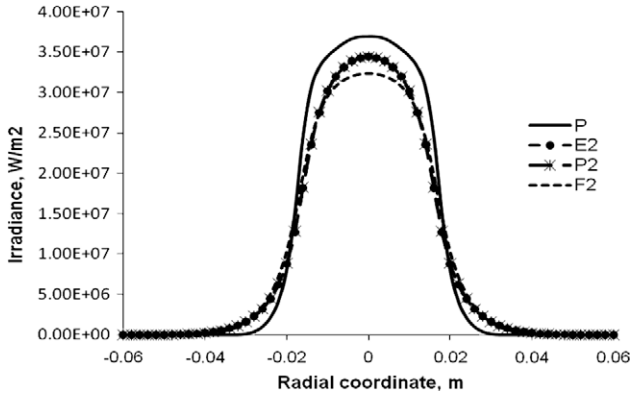

Fig. 6. Irradiance distribution in the focal plane for different frame configurations, with five groups of focal distances, as compared to a continuous paraboloid.

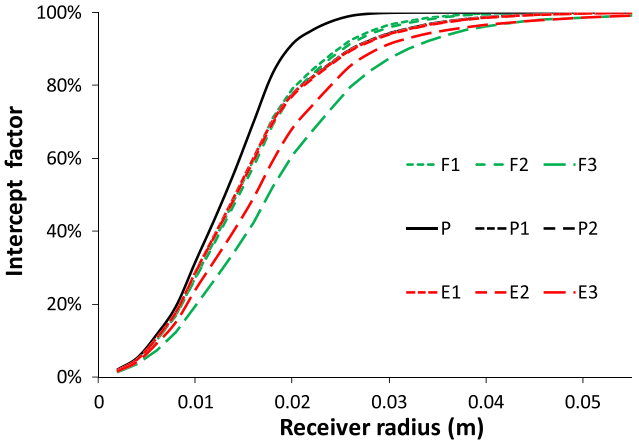

Fig. 7. Fraction of power intercepted by a flat target as a function of its radius, for the different configurations under study.

agation distances for the reflected solar cones and, consequently, more spread of the image, reducing the peak flux. Nevertheless, in the spherical and parabolic frames the most external facets are more tilted with respect to the optical axis than in the flat configurations, producing more elliptical images (spread only in one of the axes). As a consequence, the images produced by these configurations have longer limbs, even though the peak of concentration is not so strongly reduced as in the flat case.

Again in Fig. 7 we can seen that is very hard to distinguish between cases E1, E2, P1 and P2, as they largely overlap in the whole interval. The four configurations have very good performance. Of course, as pointed out above, none of the faceted configurations is as good as a continuous paraboloid, which produces more concentrated power for any given radius than the other configurations. The approximation to a continuous paraboloid by faceted concentrators improves steadily as the number of facets increases, as has been pointed out elsewhere (Riveros-Rosas et al., 2008, submitted for publication), but a higher number of smaller facets would be unpractical for the fabrication of the furnace.

According to the above results, it was determined that the case E2, spherical frame with tilted facets grouped in five different sets of focal distances is an adequate option. The next step consisted in studying the effect of the curvature radius of this frame. It was considered that a smaller radius could improve the concentration by reducing the distance travelled by the reflected solar cones, therefore limiting the spread of the solar image. In Fig. 8 the variation of peak concentration with curvature radius is presented. It is observed that the best concentration is obtained for curvature radius between 500 and 550 cm. However, the concentration factor for the studied cases has a maximum variation of only 1.3%. On the other hand, the rim angle of the concentrator increases considerably as the radius of curvature is reduced. A large rim angle may result inconvenient for the implementation of receivers in the focal zone, due to the large incidence angles of radiation, as illustrated in Fig. 9. Therefore, there seems to be very little to be gained from the reduction of the radius, and there are potential problems with this. A radius of 7.5 m was fixed for the following simulations, giving a effective focal distance of 3.68 m.

The next study was to analyze the effects of optical errors in the performance of the concentrator. For this purpose, the E2 configuration was considered. Reflectivity was taken as 0.81 and focal distances according to the previously described sets. In Fig. 10 the results are presented for peak concentration, average concentration, and spot radius (for 90% collected power). We can see that with values of the optical error between 3 and 4 mrad, the peak concentration is between 15,000 and 10,500 suns, while spot radius would be between 4 and 5 cm. So, a maximum optical error of around 4 mrad is required to meet the design targets initially established for the solar furnace. This result does not take in account the shadowing by objects in the focal zone and the shutter structure.

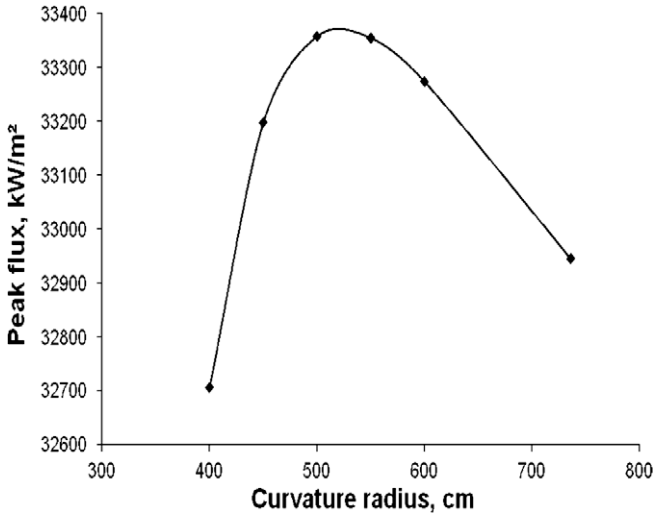

Fig. 8. Variation of peak concentration with the focal distance of the concentrator, for the E2 configuration.

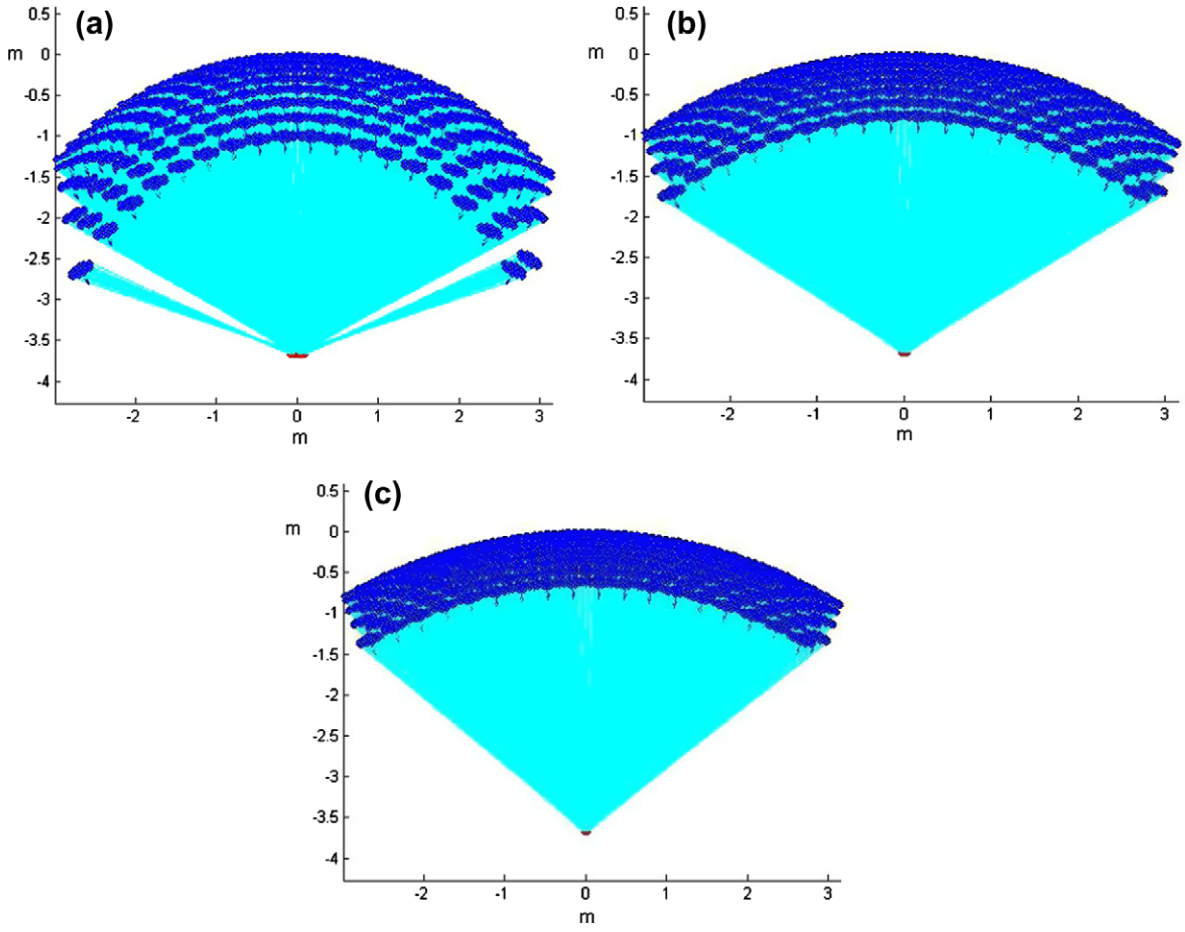

Fig. 9. Layout of the E2 configuration, with different curvature radii of the frame; (a) 4 m, (b) 5 m, and (c) 6 m.

In spite of the above remarks about the little influence of the radius of curvature of the frame on the peak concentration, it has been found that optical errors modify not only the concentration factor but also other characteristics of a faceted concentrator, like the optimal focal distance (Riveros-Rosas et al., 2008, submitted for publication). Therefore, the radius of curvature of the frame was again varied when studying the effect of optical errors. In Fig. 11, the average irradiance values for different focal distances and optical errors are presented, for a configuration of the type E2.

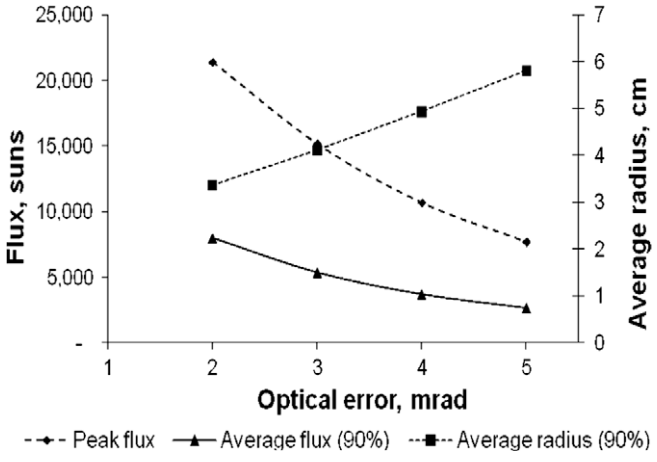

Fig. 10. Peak and average radiative flux, and radius of the spot on a flat receiver as a function of optical error.

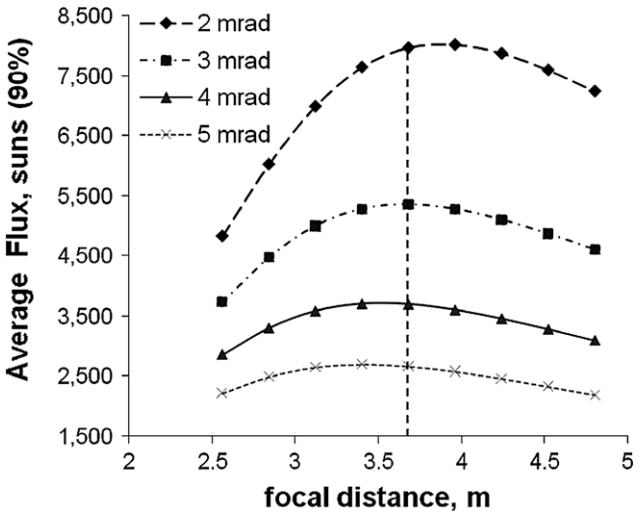

Fig. 11. Average irradiance on the receiver (90% collection) for different focal distances and optical errors. Dashed line, selected focal distance.

As can be seen from Fig. 11, even though there is a dependence of the optimal focal distance with optical error, the variation is not sharp. The previously selected focal distance of 3.68 m is well within the optimal range for the errors considered.

From all the above analysis, the final configuration chosen is a spherical frame with curvature radius equal to 7.36 m, and facets of five different focal distances, as illustrated in Fig. 12 and Table 2, giving an effective focal distance of 3.68 m. This configuration should be able to achieve a peak solar concentration of 10,500 suns and a spot radius of 5 cm, if optical errors are kept below 4 mrad.

Finally, note that the last group of mirrors (the E group) is formed by only 12 facets. In order to simplify the construction of the system, the focal length of this group can be made equal to that of group D, without important loss in performance.

It must be pointed out, that the optical error considered in the discussions above is the global error of the system. This includes the alignment and surface errors of the facets, but also the alignment, surface, curvature, and tracking errors of the heliostat. Therefore, the upper bound of 4 mrad must accommodate for all of these effects.

Actually, the type of concentrating facets considered can be fabricated with very high accuracy, resulting in a surface error very close to zero, as preliminary results show. Also, accurate alignment procedures are being developed for the facets of the concentrator, based both on the Ronchi optical test and on the use of a 3D coordinate measuring system. Therefore, it can be expected that the optical error of the concentrator can be negligible as compared to errors associated with the heliostat.

In the heliostat, tracking errors bellow 1 mrad can be achieved, and the intrinsic surface errors from the reflecting material are also small. The main sources of error are therefore expected to come from the flatness of facets, their alignment, and in general, from mechanical deformations during tracking. A specific heliostat mechanical design is in process, where the target is to minimize all these errors.

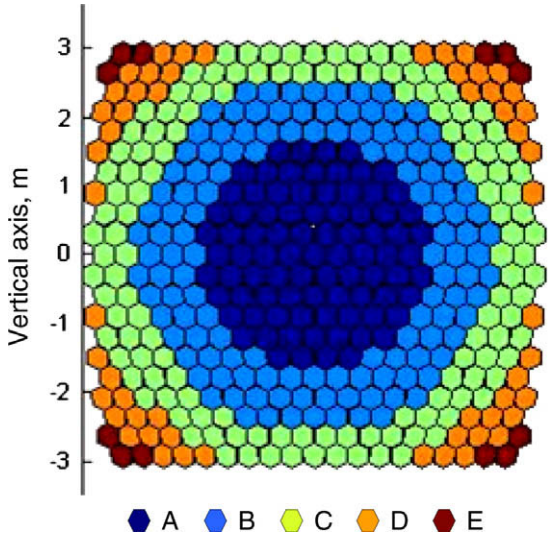

Fig. 12. Distribution of the facets of the concentrator with spherical frame in groups of equal focal distance.

Table 2
Groups of focal distances considered for the case E2.

Group	Focal distance (m)	Number of facets
A	3.75	85
B	4.00	126
C	4.25	130
D	4.50	56
E	4.75	12

5. Conclusions

The design of the HRFSF aims to create a high quality infrastructure for research in solar concentration systems in Mexico. The design considers a faceted concentrator, formed by 409 hexagonal first surface polished glass mirrors. The mirrors will be attached to a frame of spherical curvature. Ray tracing results indicate that there is very little difference in optical performance between a parabolic and a spherical frame, but the latter may be easier to fabricate. It was found that it is not convenient to use mirrors of equal focal distances, mounted tangent to the frame curvature. Instead, each mirror should have its own focal distance and tilting angle with respect to the frame. This helps compensating for the optical aberrations. It was found that grouping the mirrors in five sets of equal focal distances gives very good results. Also, the effect of optical errors was investigated. It was found that error must be kept below 4 mrad to reach the design targets.

Acknowledgements

This work was partially supported by CONACYT (Grant 56918) and UNAM (Grant 372311721). D. Riveros-Rosas and J. Herrera-Vázquez acknowledge graduate scholarships from CONACYT. J.J. Quiñones Aguilar is acknowledged for technical support.

References

Abdurakhamanov, A.A., Akbarov, R.Y., Gulamov, K.G., Riskiev, T.T., Yuldasheva, A., 1998. Operating experience of a big solar furnace 1000 kW in power. Appl. Solar Energy 34, 29–33.

Biggs, F., Vittitoe, C.N., 1979. Helios model for the optical behavior of reflecting solar concentrators. Sandia National Laboratories Report, SAND 76-0347, Albuquerque, USA.

Brenden, B.B., Newkirk, H.W., Woodcock, S.H., 1958. A study of temperature measurement in a solar furnace. Solar Energy 2, 13–17.

Buie, D., Monger, A.G., Dey, C.J., 2003. Sunshape distributions for terrestrial solar simulations. Solar Energy 74, 113–122.

Chen, Y.T., Chong, K.K., Lim, C.S., Lim, B.H., Tan, K.K., Aliman, O., Bligh, T.P., Tan, B.K., Ismail, G., 2002. Report of the first prototype

of non-imaging focusing heliostat and its application in high temperature solar furnace. Solar Energy 72, 531–544.

Estrada, C.A., Jaramillo, O.A., Acosta, R., Arancibia-Bulnes, C.A., 2007. Heat transfer analysis in a calorimeter for concentrated solar radiation measurements. Solar Energy 81, 1306–1313.

Fletcher, E.A., 2001. Solarthermal processing: a review. J. Solar Energy Eng. 123, 63–74.

Glaser, P.E., 1958. Engineering research with a solar furnace. Solar Energy 2, 7–10.

Hisada, T., Mii, H., Noguchi, C., Noguchi, T., Hukuo, N., Mizuno, M., 1957. Concentration of the solar radiation in a solar furnace. Solar Energy 1, 14–18.

Jonhnston, G., 1995. Flux mapping the 400 m^2 'Big Dish' at the Australian National University. J. Solar Energy Eng. 117, 290–293.

Kevane, C.J., 1957. Construction and operation of the Arizona State College solar furnace. Solar Energy 1, 99–101.

Lim, C.S., Li, L., 2009. Flux distribution of solar furnace using non-imaging focusing heliostat. Solar Energy 83, 1200–1210.

Loh, E., Hiester, N.K., Tietz, T.E., 1957. Heat flux measurements at the sun image of the California institute of technology lens-type solar furnace. Solar Energy 1, 23–26.

Neumann, A., Groer, U., 1996. Experimenting with concentrated sunlight using the DLR solar furnace. Solar Energy 58, 181–190.

Pérez-Rábago, C.A., Marcos, M.J., Romero, M., Estrada, C.A., 2006. Heat transfer in a conical cavity calorimeter for measuring thermal power of a point focus concentrator. Solar Energy 80, 1434–1442.

Rabl, A., Bendt, P., 1982. Effect of circumsolar radiation on performance of focusing collectors. J. Solar Energy Eng. 104, 237.

Riveros-Rosas, D., Sanchez-Gonzalez, M., Arancibia-Bulnes, C., Estrada, C., 2008. Influence of the Size and Number of Facets on Point Focus Concentration Systems. EUROSUN Congress, Lisbon, Portugal, October 7–10, 2008.

Riveros-Rosas, D., Sanchez-Gonzalez, M., Arancibia-Bulnes, C.A., Estrada, C.A., submitted for publication. Influence of the size of facets on point focus solar concentrators. Renewable Energy.

Romero, V.J., 1984. CIRCE2/DEKGEN2: A Software Package for Facilitated Optical Analysis of 3-D Distributed Solar Energy Concentrators. Sandia National Laboratories Report, SAND91-2238, Albuquerque, USA.

Schubnell, M., Kelle, J., Imhof, A., 1991. Flux density distribution in the focal region of a solar concentrator system. J. Solar Energy Eng. 113, 112–116.

Trombe, F., Le Phat Vinh, A., 1973. Thousand kW solar furnace, built by the National Center of Scientific Research, in Odeillo (France). Solar Energy 15, 57–61.